Metabolic Engineering **4**, 248–256 (2002)
doi:10.1006/mben.2002.0230

Metabolic Flux Analysis of *Candida tropicalis* Growing on Xylose in an Oxygen-Limited Chemostat

Tom Granström,*[,1] Aristos A. Aristidou,[†] and Matti Leisola*

[*] *Laboratory of Bioprocess Engineering, Helsinki University of Technology, P.O.B. 6100, Kemistintie 1, FIN-02015 HUT, Finland; and*
[†] *Cargill Dow LLC, Minnetonka, Minnesota 55345*

Received October 22, 2001; accepted May 9, 2002

We have studied the metabolism of xylose by *Candida tropicalis* in oxygen-limited chemostat. *In vitro* enzyme assays indicated that glycolytic and gluconeogenetic enzymes are expressed simultaneously facilitating substrate cycling. Enhancing the redox imbalance by cofeeding of formate increased xylose and oxygen consumption rates and ethanol, xylitol, glycerol and CO_2 production rates at steady state. Metabolic flux analysis (MFA) indicated that fructose 6-phosphate is replenished from the pentose phosphate pathway in sufficient amounts without contribution of the gluconeogenetic pathway. Substrate cycling between pyruvate kinase, pyruvate carboxylase and phospho-*enol*-pyruvate kinase increased ATP turnover. Cofeeding of formate increased the ATP yield. The ATP yields of xylose and xylose–formate cultivation were 6.9 and 8.7 mol ATP/C-mol CDW, respectively, as calculated from the MFA. © 2002 Elsevier Science (USA)

***Key Words: Candida tropicalis*; metabolic flux analysis; formate; cofeeding; oxygen limitation; chemostat; substrate cycling.**

INTRODUCTION

Metabolic flux analysis (MFA) can be used for identification of branch points of pathways or calculation of nonmeasured extracellular fluxes or calculation of maximum theoretical yields (Stephanopoulos *et al.*, 1998). MFA facilitates analysis and more importantly comparison of large sets of data in different conditions. However, the information obtained is always dependent on matrix constraints. One disadvantage of MFA is that intracellular substrate cycling and equilibrium reactions are difficult to model without running into singularity problems in matrix calculations. If only the main pathways are included in the metabolic network the results may be self-explanatory. Furthermore, it is impossible to extend the applicability of stoichiometric modelling in calculating the cofactor balances for, e.g., ATP, NADH or NADPH. For studying intracellular fluxes a number of different methods have been used. These include mass spectrometry with MFA (Wittman and Heinzle, 1999), NMR spectroscopy (Petersen *et al.*, 2000; Frey *et al.*, 2001; Schmidt *et al.*, 1999; de Graaf *et al.*, 1999) and MFA and/or *in vitro* enzyme assays (Vallino and Stephanopoulos, 1993; Nissen *et al.*, 1997; van Gulik and Heijnen, 1995; de Jong-Gubbels *et al.*, 1996; van Hoek *et al.*, 1998).

The significance of redox balances on substrate uptake in yeast xylose metabolism has been studied thoroughly (Hallborn *et al.*, 1994; Jeppsson *et al.*, 1999; Kötter and Ciriacy, 1993). The effect of redox balance on metabolite production is evident (Zupke *et al.*, 1995; Vandeska *et al.*, 1995; Oh *et al.*, 1998; Gìrio *et al.*, 1994). Flikweert *et al.* (1999) concluded that glycolytic flux is controlled by NADH reoxidation by pyruvate decarboxylase. Porro *et al.* (1999) introduced a lactate dehydrogenase gene into a deletion strain of *Kluyveromyces lactis*. The result was that lactic fermentation substituted completely the ethanol production pathway. Linearly deepening oxygen limitation resulted in increased intracellular NADH concentration and that led to an increased rate of xylitol production by *Candida guilliermondii* (Granström *et al.*, 2001). To study the effects of additional intracellular NADH on cell metabolism formate can be used as a cosubstrate (Bruinenberg *et al.*, 1983, 1985). Formate produces NADH and CO_2 in an NAD-dependent formate dehydrogenase (FDH) catalysed reaction. The produced NADH can be used as an energy source, but CO_2 is not a carbon source for *Candida utililis* (Bruinenberg *et al.*, 1983).

C. tropicalis is industrially important, because of its high xylose uptake rate and xylitol production capacity. However, its physiology has not been studied extensively in defined conditions. It has no sexual stage (Barnett *et al.*, 1983), which may present problems in developing genetic tools. Furthermore, its morphology changes from mycelium culture to single-cell culture according to oxygen

[1] To whom correspondence and reprint requests should be addressed. Fax: +358-0-462 373. E-mail: tom.granstrom@hut.fi.

0022-4596/02 $35.00

Metabolic Engineering **4**, 248–256 (2002)
doi:10.1006/mben.2002.0230

availability in the chemostat (Granström, unpublished results). In this work we have studied the metabolism of *C. tropicalis* in oxygen-limited chemostat under high xylose concentration. The oxygen-limited steady states were established when the xylitol production rate was highest. In these conditions ethanol and glycerol were also produced, and residual xylose accumulated, which confirmed the oxygen limitation. *In vitro* enzyme assays and metabolic flux analysis (MFA) were used to study the intracellular fluxes influencing xylitol production. Formate was used as a cosubstrate to increase the intracellular concentration of NADH. We hypothesised that excess NADH would result in higher oxygen and xylose consumption and correspondingly increase xylitol production by inhibiting xylitol dehydrogenase enzyme.

Metabolic flux analysis was based on a previously published model that took into consideration cell compartmentalisation and shuttling of substrates across the mitochondrial membrane (Granström *et al.*, 2000). In the present model we have further emphasised substrate cycling between cytosol and mitochondria. This approach enabled us to study the effects of different metabolic pathways implicated by *in vitro* enzyme assays on ATP yield in xylose and xylose–formate cultivations.

MATERIALS AND METHODS

Organism, Maintenance and Inoculum Preparation

Candida tropicalis VTT-C-78086 (ATCC 1369) was obtained from VTT Biotechnology (Espoo, Finland). Frozen stock cultures containing 20% (w/v) glycerol were stored in 2 ml ampoules at -70°C. Inoculum for fermentation was prepared in 250 ml shake flasks grown overnight on YPD-medium at 30°C and 200 rpm. YPD-medium contained 10 g/L yeast extract (Difco), 20 g/L bactopeptone (Difco) and 20 g/L glucose (Fluka).

Chemostat Experiments

Mineral medium was prepared according to Verduyn *et al.* (1992). The medium contained per litre: $(NH_4)_2SO_4$ 5.0 g, KH_2PO_4 3.0 g, $MgSO_4 \cdot 7H_2O$ 0.5 g, EDTA 15 mg, $ZnSO_4 \cdot 7H_2O$ 4.5 mg, $CoCl_2 \cdot 6H_2O$ 0.3 mg, $MnCl_2 \cdot 4H_2O$ 1 mg, $CuSO_4 \cdot 5H_2O$ 0.3 mg, $CaCl_2 \cdot 2H_2O$ 4.5 mg, $FeSO_4 \cdot 7H_2O$ 3 mg, $Na_2MoO_4 \cdot 2H_2O$ 0.4 mg, H_3BO_4 1 mg, KI 0.1 mg and silicon-based antifoam agent 0.05 mg (BDH). All the medium components were doubled due to the high concentration of xylose in the medium. Mineral medium was autoclaved for 20 min at 120°C. After autoclaving a filter-sterilised vitamin solution was added giving a final concentration per litre of biotin 0.05 mg, calcium pantothenate 1 mg, nicotinic acid 1 mg, *myo*-inositol 25 mg, pyridoxal hydrochloride 1 mg and *para*-aminobenzoic acid 0.2 mg. Xylose was sterilised at 110°C for 20 min and added separately to the growth medium in order to give a final concentration of 50 g/L (1.67 C-mol/L). Culture purity was monitored on a regular basis by phase contrast microscopy. The formic acid solution was prepared by adding formic acid aseptically to an autoclaved solution to a final concentration of 115 g/L (2.5 C-mol/L).

Chemostat cultivations were carried out in a 2-litre fermenter (Braun MD) on a mineral medium at 30°C and the culture pH was set at 5.0 and it was kept constant by the addition of 2 M KOH. The working volume of 1000 ml was kept constant by removing the effluent with a peristaltic pump (Watson-Marlow 505U) that was connected to a PID-controlled load cell. The actual working volume was determined at the end of each experiment. The air flow rate was set to 0.888 L/min and it was controlled using a massflow controller (Bronkhurst HiTec, Ruurlo, Holland). The dissolved oxygen concentration was measured with O_2-electrode (Ingold). The oxygen-limited chemostat was created by agitation speed and dilution rate profiles. The agitation speed was decreased from 2000 to 866 rpm simultaneously with increasing dilution rate profile from 0.1 to 0.27 h^{-1} within 5 h and the culture was let to reach a steady state. These conditions were chosen based on the highest xylitol production rate. Five volume changes were allowed to take place to ensure steady-state conditions. Cofeeding of formate was done with a peristaltic pump (Watson-Marlow 101U), which was controlled by a central unit of the Braun MD fermenter.

Exhaust Gas Analysis

The fermentation exhaust gas was cooled to 4°C in a condenser to prevent the evaporation of volatile compounds before entering into the masspectrometer (VG-Prima 600). Carbon dioxide, oxygen, argon and nitrogen were analysed from exhaust gas. There was no overpressure in the reactor. In calculating the oxygen consumption rates and carbon dioxide production rates temperature of 30°C was assumed and air pressure was taken from the daily weather report.

Cell Dry Weight Measurements

Culture samples (5 ml) were vacuum filtered through preweighed nitro-cellulose filters (0.45 μm, Schleicher & Schuell), washed with Milli-Q water and then dried in a microwave oven for 20 min (Ignis, Japan).

Substrate and Metabolite Analysis

Samples (1.2 ml) from the chemostat were centrifuged at 8000*g* for 5 min (Heraeus Sepatech, Biofuge A, Germany) and the supernatant was analysed contemporaneously. Xylose, formate, xylitol, glycerol, acetate and ethanol concentrations were analysed by HPLC. The set-up included an HPX-87H Aminex ion-exclusion column (Bio-Rad) and two detectors in series, a Waters 410 refractive index and a Waters 486 UV-detector (214 nm). The column was maintained at 60°C and eluted with 5 mM H_2SO_4 at a flow rate of 0.6 ml/min.

Metabolic Flux Analysis

Modifications to our previously published metabolic flux analysis (Granström *et al.*, 2000) are presented in Appendix 1. The oxygen-limited xylose cultivation model contained 99 compounds and 85 reactions and the xylose-formate cultivation contained 101 compounds and 87 pathway reactions. Specific consumption of xylose, formate, oxygen and production of xylitol, glycerol, acetate, ethanol, carbon dioxide and biomass was measured. The accumulation of protein, lipids, RNA, polysaccharides and amino acids were according to the previous model. All other metabolites were assumed to be at pseudo-steady-state (PSS), i.e. the net accumulation rates are equal to zero. Compared to the earlier published model (Granström *et al.*, 2000) the transport of ions and ATP consumption for maintenance energy (r_{39}) has been lumped. Furthermore, xylitol dehydrogenase (XDH) and xylulokinase (XK) (r_4) fluxes have been lumped. In addition, phosphofructokinase reaction is removed and gluconeogenetic fluxes have been added (r_6 and r_7). Finally, the reactions of formate catabolism (r_{42} and r_{43}) have been added. In all simulations the xylose and formate consumption rates were constrained to use all the available carbon substrate. Simulations were carried out where phosphoglucoisomerase (PGI), pyruvate kinase (PK), fructose 1,6-bisphosphatase (F16BP) and phospho-*enol*-pyruvatecarboxykinase (PEPCK) were constrained to zero one at a time. The impact of deleting these fluxes on ATP yield was calculated with MFA. In ATP yield calculations the PO value of 1.0 for NADH oxidation and 0.1 for FADH oxidation was applied. In all cases the matrices were full rank and the solution was found by a constrained linear least-squares (CONLS) method by MATLAB (The MathWorks Inc.). The metabolic network was constructed by Mathcad 2000 Professional (MathSoft Inc).

Preparation of Cell-Free Extract

Cell-free extract was prepared according to de Jong-Gubbels *et al.* (1996) with the exception that cells were disrupted with Vibra Cell sonicator (VCX600, USA). Ten 30 s pulses were applied with 30 s cooling period between each pulse.

Enzyme Assays

Enzyme assays were performed at 30°C with freshly prepared cell-free extracts using a Shimadzu UV-2100 spectrophotometer. Reaction rates, corrected for endogenous rates, were proportional to the amount of extracts added. Xylose reductase (XR, EC 1.1.1.21) and xylitol dehydrogenase (XDH, EC 1.1.1.9) were assayed as described by Verduyn *et al.* (1985). Pyruvate carboxylase (PYC, EC 6.4.1.1), phospho-*enol*-pyruvate carboxykinase (PEPCK, EC 4.1.1.32), fructose-1.6-bisphosphatase (F16BP, EC 3.1.2.11), malate synthase (MS, EC 4.1.3.2) and pyruvate kinase (PK, EC 2.7.1.40) were measured according to de Jong-Gubbels *et al.* (1996). Pyruvate decarboxylase (PDC, EC 4.1.1.1), glucose-6-phosphate dehydrogenase (G6PDH, EC 1.1.1.49), alcohol dehydrogenase (ADH, EC 1.1.1.1) and NAD- (ALD, EC 1.2.1.4) and NADP-dependent (ALD, EC 1.2.1.5) acetaldehyde dehydrogenases were assayed as described by Postma *et al.* (1989). Malate dehydrogenase (MDH, EC 1.1.1.37), phosphoglucoisomerase (PGI, EC 5.3.1.9), NAD-dependent (IDH, EC 1.1.1.41) and NADP-dependent (IDP, EC 1.1.1.42) isocitrate dehydrogenase and malic enzyme (ME, EC 1.1.1.39) were measured according to Bergmeyer (1985). Formate dehydrogenase (FDH, EC 1.2.1.2) was measured according to Bruinenberg *et al.* (1983). One unit of activity is defined as the amount of enzyme catalysing the conversion of one μmol substrate per minute. Specific activities are expressed as units per mg protein.

Protein Determination

The protein content of whole cells was assayed by a modified biuret method (Verduyn *et al.*, 1990) and with the Bio-Rad protein assay kit. The protein concentration in cell-free extracts was determined by the Lowry method using BSA (Sigma) as a standard.

RESULTS

The results of the oxygen-limited chemostat and the effect of formate on *C. tropicalis* metabolism are presented in Table 1. The dilution rate of xylose was 0.27 h^{-1} in both cultivations and for the cosubstrate formate it was 0.0012 h^{-1} in the xylose–formate cultivation. The residual xylose concentration was 647 C-mmol/L (19 g/L) in the xylose cultivation. In the subsequent xylose–formate cultivation, the residual xylose and formate

Metabolic Engineering **4**, 248–256 (2002)
doi:10.1006/mben.2002.0230

TABLE 1

The Consumption and Production Rates of *Candida tropicalis* in the Oxygen-Limited Chemostat Under High Xylose Concentration

Run	Xylose (C-mmol/C-mol CDW/h)	Biomass (C-mmol/C-mol CDW/h)	Formate (C-mmol/C-mol CDW/h)	$q(O_2)$ (mmol/C-mol CDW/h)	$q(CO_2)$ (C-mmol/C-mol CDW/h)	Xylitol (C-mmol/C-mol CDW/h)	Glycerol (C-mmol/C-mol CDW/h)	Ethanol (C-mmol/C-mol CDW/h)	Carbon balance (%)
Xylose (control)	774	268		202	246	149	3.4	81	98
Xylose–formate	842	274	4.8	231	271	160	4.8	99	98

Note. The cultivations were done at 30°C on a mineral medium at pH 5. The dilution rate for xylose was 0.27 h^{-1} in both cultivations and for cosubstrate formate it was 0.0012 h^{-1} in xylose–formate cultivation.

concentrations were 863 C-mmol/L (26 g/L) and 7.0 C-mmol/L (0.32 g/L), respectively. In the xylose cultivation the specific xylose consumption q(xyl) was 774 C-mmol/C-mol CDW/h. The cofeeding of formate increased the q(xyl) to 842 C-mmol/C-mol CDW/h. The specific oxygen consumption (qO_2) and carbon dioxide production rates (qCO_2) increased correspondingly. Also, the specific xylitol, ethanol and glycerol production rates increased. However, the specific production of biomass $q(x)$ did not increase significantly due to cofeeding of formate. In all steady states the carbon balance was closed with 98% accuracy.

The results of the *in vitro* enzyme assays are presented in Table 2. The enzyme assays were carried out to study the xylose metabolism of *C. tropicalis* and the effects of the formate cofeeding under oxygen-limited conditions. The enzyme assays indicated that xylose reductase (XR) has a dual dependency for NADPH and NADH during formate feeding. Small, but consistent NADH-dependent activity was found from the xylose cultivation also. Glucose 6-phosphate dehydrogenase (G6PDH) activity was found from both cultivations indicating that NADPH was generated primarily through pentose phosphate pathway (PPP). In addition, G6PDH has a significant role also in trehalose and glycogen synthesis (Francois and Parrou, 2001). Both NAD- and NADP-dependent activities of isocitrate dehydrogenase (IDH) were found, but the malate synthase (MS) activity was not. This indicates that glyoxylate cycle was not active under these conditions, whereas TCA cycle was. Formate dehydrogenase (FDH) activity was detected in both cultivations. We expected to find FDH activity only with xylose–formate cultivations. However, the cells were already exposed to formate feeding in earlier chemostat runs, where different dilution rates for xylose and formate were screened. Malic enzyme (ME) was found to be active with both NADH and NADPH, whereas malate dehydrogenase (MDH) was exclusively NAD-dependent. Expression of both of these enzymes at the same time enables substrate cycling, where NADPH can be converted to NADH or *vice versa* according to the *in vivo* metabolism of *C. tropicalis* (Fig. 1). Only traces of phosphoglucoisomerase (PGI), pyruvate kinase (PK), phospho-*enol*-pyruvate carboxykinase (PEPCK) and fructose 1,6-bisphosphatase (F16BP) activities were detected from both cultivations (results not shown). However, the gluconeogenic pathway (GNP) should be active in these conditions in order to synthesise storage carbohydrates and NADPH for biomass synthesis. Low activities of pyruvate carboxylase (PYC), pyruvate decarboxylase (PDC), alcohol dehydrogenase (ADH) and acetaldehyde dehydrogenase (ALD) were found from both cultivations. The expression of PK, PYC and PEPCK simultaneously facilitates increase in ATP turnover in these oxygen-limited conditions (Fig. 1).

TABLE 2

The Steady-State *In Vitro* Enzyme Activities of *Candida tropicalis* under High Xylose Concentration and Oxygen Limitation

		Activity (U/mg protein)	
Enzyme	Cofactor	Xylose	Xylose–formate
XR	NADPH	0.82	0.73
XR	NADH	0.002	0.01
XDH	NAD	0.32	0.45
G6PDH		1.1	1.0
PYC		0.02	0.04
PDC		0.02	0.05
ADH		0.03	0.02
ALD	NAD	0.05	0.06
ALD	NADP	0.00	0.01
ME	NAD	0.44	0.37
ME	NADP	0.09	0.07
IDH	NAD	0.15	0.15
IDH	NADP	0.17	0.14
MDH	NADH	13.8	12.2
FDH	NAD	0.05	0.09

Note. The activities were determined from the xylose and xylose–formate grown cells. All the measurements were done in duplicates.

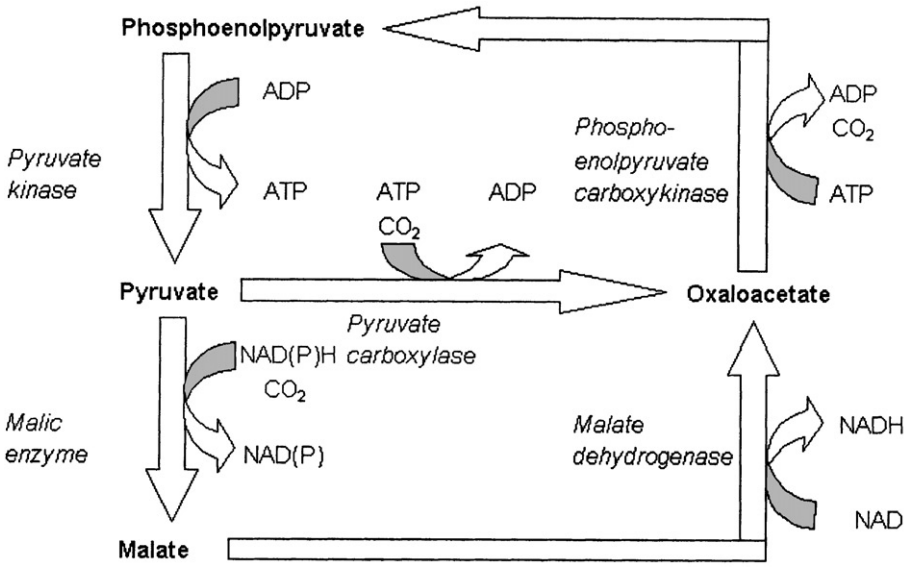

FIG. 1. Simultaneous expression of pyruvate kinase (PK), pyruvate carboxylase (PYC) and phospho-*enol*-pyruvate carboxylase (PEPCK) enables substrate cycling, which increases ATP turnover. Similarly, when malic enzyme (ME) and malate dehydrogenase (MDH) are expressed at the same this creates an transhydrogenase cycle, where NADPH is converted to NADH. Also, ME can function as a redox sink for cytosolic NADH. Malate allows alternative way for pyruvate to across the mitochondrial membrane.

Results of the metabolic flux analysis (MFA) are presented in Fig. 2. Generally, flux into pentose phosphate pathway (PPP), the upper part of the glycolytic flux and the gluconeogenetic flux were increased, whereas the TCA cycle fluxes from acetyl CoA (r_{22}) to succinate (r_{28}) is markedly reduced in the xylose–formate cultivation. Biomass (r_{41}) synthesis decreased on xylose–formate grown cells, which is in accord with the measured results. The model shows that fructose 6-phosphate (r_{37} and r_{38}) is replenished from PPP in sufficient amounts for synthesis of storage carbohydrates (r_{40}) and generation of NADPH (r_{33}). Subsequently, the F16BP flux (r_6) is close to zero. Also, ME has a negative flux resulting in malate (r_{31}), which crosses the mitochondrial membrane and is used in the mitochondria by MDH and fumarate hydratase (FHT). Simultaneous expression of ME and MDH creates an alternative way for pyruvate to cross the mitochondrial membrane in the form of malate. Therefore, substrate cycling acts as a redox sink for cytosolic NADH and generates mitochondrial NADH (Fig. 1). Oxaloacetate/aspartate shuttle (r_{23}) transports oxaloacetate over the mitochondrial membrane, which is then used by PEPCK (Fig. 1). Ethanol is converted into acetaldehyde in cytosol (r_{16}) by cytosolic ADH. Acetaldehyde diffuses into mitochondria and is converted into ethanol by mitochondrial ADH (r_{32}). Ethanol diffuses freely across the mitochondrial membrane. This substrate cycling through mitochondrial membrane regenerates cytosolic NADH and acts as a redox sink for mitochondrial NADH (Fig. 2).

In order to substantiate the results of the enzyme assays the fluxes of PGI (r_5), PK (r_{12}), F16BP (r_6) and PEPCK (r_7) were constrained to zero one at a time from the metabolic network and their effect on ATP yield was calculated (Table 3). If PK or PEPCK fluxes are constrained to zero the ATP yield will reduce approximately 60% in both cases and cultivations (Table 3). This was considered as a nonfeasible solution. When PGI flux is constrained to zero the PPP flux (r_{33}) will become negative in both cultivations. The highest ATP yield was obtained, when F16BP flux (r_6) was constrained to zero in both cultivations. Theoretically this is a feasible solution and it is in accord with the measured results: only traces of F16BP activity were found. If all these enzymes are expressed and active under these conditions (as in Fig. 1) the ATP yield of xylose and xylose–formate cultivations are 6.9 and 8.7 mol ATP/C-mol CDW, respectively.

DISCUSSION

Here we present a new method for combining the advantages of *in vitro* enzyme assays and metabolic flux analysis. For the first time the intracellular fluxes under oxygen limitation and high xylose concentration in the chemostat have been modelled demonstrating intracellular

Metabolic Engineering **4**, 248–256 (2002)
doi:10.1006/mben.2002.0230

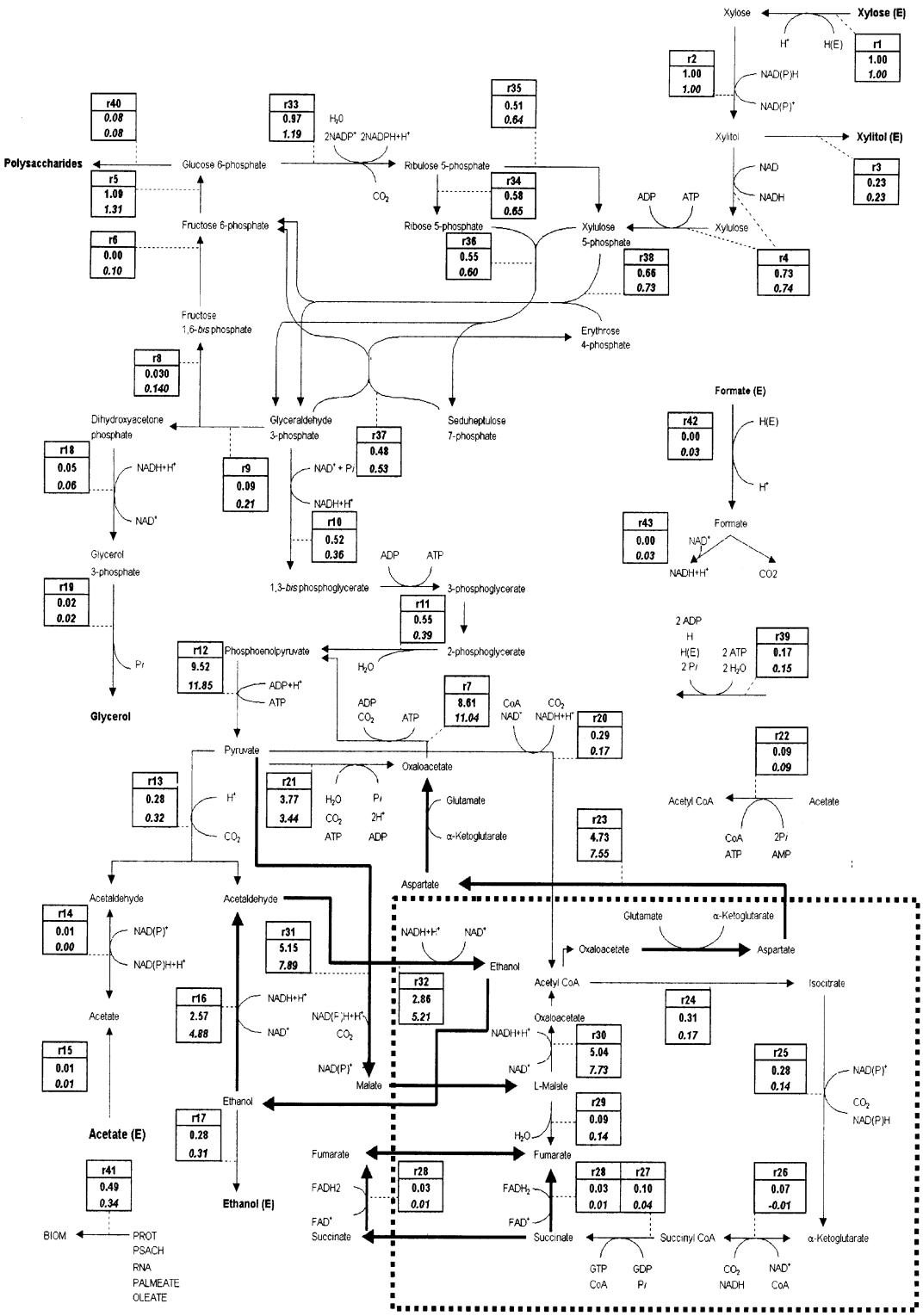

FIG. 2. The steady-state fluxes of *Candida tropicalis* in oxygen limited chemostat. The boxes indicate the reaction number referred to in the text and the flux value of xylose cultivation and xylose–formate cultivation (italics). All the fluxes are indicated by arrow direction. The fluxes are presented in mmol/L/h and they are normalised according to the xylose uptake rate. The dotted line represents mitochondrial membrane. The shuttling of substrates over the mitochondrial membrane is depicted with bold arrows.

TABLE 3

The ATP Yields of Xylose and Xylose–Formate Cultivations Calculated by Metabolic Flux Analysis (MFA)

Cultivation	$Y \times$ ATP (mol ATP/C-mol CDW)				
	Control	PGI = 0	PK = 0	F16BP = 0	PEPCK = 0
Xylose	6.9	3.6	2.2	6.9	2.9
Xylose–formate	8.7	4.9	2.3	8.1	3.1

Note. Different simulations were carried out by constraining phosphoglucoisomerase (PGI), pyruvate kinase (PK), fructose 1,6-bisphosphatase (F16BP) and phospho-*enol*-pyruvate carboxykinase (PEPCK) fluxes to zero one at a time from the metabolic network. Control refers to the cultivation where all the PGI, PK, F16BP and PEPCK were expressed (Fig. 1). The ATP yield ($Y \times$ ATP) is expressed as mol ATP/C-mol CDW.

substrate cycling. In this study we have shown that different competing metabolic pathways in *C. tropicalis* can function simultaneously and in highly uneconomical ways in these conditions. When *in vitro* enzyme assays are used exclusively, the results should be interpreted with care. Also, the metabolic flux analysis should not be taken as a reflection of *in vivo* metabolism. The advantage of combining MFA with *in vitro* enzyme assays, in this study, is that it points out the possible metabolic flux distribution in respect to ATP generation. In addition, it allows comparison of different growth conditions. The method we have applied demonstrated three intracellular substrate cycles between (1) pyruvate carboxylase (PYC), pyruvate kinase (PK) and phospho-*enol*-pyruvate carboxykinase (PEPCK), (2) malate dehydrogenase (MDH) and malic enzyme (ME) (3) cytosolic and mitochondrial alcohol dehydrogenase (ADH) and aldehyde dehydrogenase. The measured activities of MDH, ME and PYC were consistent with the model, but the results of PK and PEPCK enzyme assays cannot be interpreted as straightforwardly.

The ATP yield calculation by MFA was used to justify the presence of PK and PEPCK. Excluding these fluxes from the metabolic network decreased the ATP yield by almost 60%. The calculated ATP yield in xylose culture was 6.9 mol ATP/C-mol CDW (276 mmol ATP/g CDW), and in xylose–formate culture 8.7 mol ATP/C-mol CDW (349 mmol ATP/g CDW). For ethanol grown *C. utilis* the ATP yield of 106 mmol ATP/g CDW has been reported (Verduyn *et al.*, 1991). Higher ATP yield in xylose–formate cultivation is explained by additional energy source of formate catabolism. Glycolytic flux increased with deepening redox imbalance resulting in higher specific xylose consumption and xylitol, ethanol and glycerol production (Table 1). Formate cofeeding resulted in large disruption of xylose metabolism. Primarily, this was due to the dual effect of additional NADH on xylose metabolism. Firstly, it facilitates xylose reduction into xylitol by XR by generating NADH. Secondly, the surplus of NADH inhibits the XDH activity resulting in xylitol excretion. Eventually, formate will inhibit the growth of the yeast cells by dissipating the proton motive force of the cell and results in washout (Granström and Leisola, 2002). The highest measured formate consumption rate was 4.8 C-mmol/C-mol CDW/h. Formate produces NADH and CO_2 in 1:1 molar ratio. However, the CO_2 production increased 25 C-mmol/C-mol CDW/h compared to the xylose cultivation. *C. tropicalis* was unable to assimilate the CO_2 produced by FDH into biomass synthesis; thus $q(x)$ increased only 2%, which is in the limits of experimental error. It could be speculated that one of the carboxylating reactions (PYC, ME) would be able to use the CO_2 generated by formate catabolism, but this question remains to be solved by isotope labelling studies.

Ethanol is metabolised through glyoxylate cycle and gluconeogenesis, whereas xylose uses PPP and gluconeogenesis. The glyoxylate cycle was inactive on xylose and xylose–formate according to the *in vitro* MS activity. Only traces of gluconeogenetic pathway enzyme activities (F16BP, PEPCK) could be measured. The MFA showed that the flux of F16BP (r_6) is close to zero. MFA simulation showed that ATP yield increased, when F16BP flux was constrained to zero. Gancedo and Delgado (1984) showed that mutants lacking the F16BP activity were unable to grow on any gluconeogenic carbon source; however, the growth conditions are not comparable with this study. Fructose 2,6-bisphosphate (F26BP) derived from FRU6P is a signal molecule, which activates PFK and inhibits F16BP (van Schaftingen *et al.*, 1980). This cycling between PFK and F16BP activities is possible in these conditions, also. Distinctive G6PDH activity was found in this study, but no phosphoglucoisomerase activity. The MFA indicated that FRU6P is replenished from PP-pathway in sufficient amount to fulfill the requirements of polysaccharide synthesis and NADPH generation by G6PDH. The product of F16BP activity (F1.6bP) is a potent activator of pyruvate kinase. This suggests that gluconeogenic enzymes are expressed in these conditions, but the FRU6P flux from PPP and not via F16BP allows also pyruvate kinase activity.

In this work we have studied the metabolic fluxes under oxygen limitation and high substrate concentration in the chemostat. The level of the oxygen limitation was chosen based on the highest xylitol production rate in these conditions. The *in vitro* enzyme assays showed that in these conditions the normal enzyme regulation is disturbed and substrate cycling is possible. The results of the enzyme assays were substantiated with metabolic flux analysis.

Metabolic Engineering **4**, 248–256 (2002)
doi:10.1006/mben.2002.0230

The MFA points to an alternative way of increasing ATP turnover through substrate cycling (Fig. 1). Malate was shown to act as a cytosolic redox sink for NADH and facilitating a transhydrogenase cycle. Similarly, acetaldehyde acted as a redox sink for mitochondrial NADH. When xylose serves as a carbon source pentose phosphate pathway (PPP) and gluconeogenic pathway (GNP) has to be active in order to synthesise storage carbohydrates and NADPH. MFA showed that FRU6P is replenished from the PPP in sufficient amounts, which may reduce the role of GNP as a glucose synthesising pathway.

ACKNOWLEDGMENT

Danisco Ltd. is acknowledged for financial support.

APPENDIX 1

The reactions, which are added or modified compared to earlier published MFA (Granström *et al.*, 2000), are given in this appendix.

1. Xylose metabolism—Xylose reductase (XR)
   $\text{Xylose} + a_2\text{NADPH}_2\text{cyt} + (1 - a_2)\text{NADH}_2\text{cyt} \rightarrow \text{Xylitol} + a_2\text{NADP} + (1 - a_2)\ \text{NAD}$ Xylose cultivation $a_2 = 1.0$; xylose–formate cultivation $a_2 = 0.98$ (coefficient a refers to the experimentally measured cofactor dependency) (cyt = cytosolic)
2. Xylose metabolism—Xylitol production
   $\text{Xylitol} \rightarrow \text{Xylitol (extracellular)}$
3. Xylose metabolism—Xylitol dehydrogenase (XDH) and xylulose kinase (XK)
   $\text{Xylitol} + \text{ATP} + \text{NAD} \rightarrow \text{Xylulose-5-P} + \text{ADP} + \text{NADH}$
4. Gluconeogenesis—Fructose 1,6-bisphosphatase (F16BP)
   $\text{Fructose 1,6-bisphosphate} + \text{H}_2\text{O} \rightarrow \text{Fructose 6-phosphate} + \text{P}_i$
5. Gluconeogenesis—Phospho-*enol*-pyruvate carboxykinase (PEPCK)
   $\text{OAC (cyt)} + \text{ATP} \rightarrow \text{PEP} + \text{ADP} + \text{CO}_2$
6. Glycolysis—Acetate production
   $\text{Acetate} \rightarrow \text{Acetate (extracellular)}$
7. Glycolysis—Ethanol production
   $\text{EtOH} \rightarrow \text{EtOH (extracellular)}$
8. TCA—Isocitrate dehydrogenase (IDH)
   $\text{Isocitrate (mit)} + (1 - a_{25})\text{NADP} + a_{25}\text{NAD} \rightarrow \alpha\text{-ketoglutarate} + \text{CO}_2 + (1 - a_{25})\text{NADPH}_2\text{cyt} + a_{25}\text{NADH}_2\text{mit}$
   (Xylose cultivation $a_{25} = 0.5$; xylose–formate cultivation $a_{25} = 0.5$) (mit = mitochondrial)
9. TCA—Malic enzyme (ME)
   $\text{MAL} + a_{31}\text{NAD} + (1 - a_{31})\text{NADP} \rightarrow \text{PYR} + a_{31}\text{NADH}_2\text{cyt} + (1 - a_{31})\text{NADPH}_2\text{cyt} + \text{CO}_2$
   (Xylose cultivation $a_{31} = 0.8$; xylose–formate cultivation $a_{31} = 0.8$)
10. TCA—Mitochondrial ethanol dehydrogenase (ADHmit)
    $\text{Acetaldehyde} + \text{NADH}_2\text{mit} + \text{H} \rightarrow \text{EtOH} + \text{NAD}$
11. Transport of ions—H + ATPase and maintenance
    $2\text{ATP} + 2\text{H}_2\text{O} \rightarrow 2\text{ADP} + \text{H (extracellular)} + \text{H} + 2\text{P}_i$
12. Formate metabolism—Uptake of formate
    $\text{Formate (extracellular)} \rightarrow \text{Formate} + \text{H}$
13. Formate metabolism—Formate dehydrogenase (FDH)
    $\text{Formate} \rightarrow \text{NADH}_2\text{cyt} + \text{CO}_2$

REFERENCES

Barnett, J. A., Payne, R. W., and Yarrow, D. (1983). "Yeasts Characteristics and Identification," Cambridge Univ. Press, Cambridge, UK.

Bergmeyer, J. (1985). "Methods of Enzymatic Analysis," 3 edn., Vols. II and III, Verlag Chemie, Weinheim, Deerfield Beach.

Bruinenberg, P. M., van Dijken, J. P., and Scheffers, W. A. (1983). An enzymic analysis of NADPH production and consumption in *Candida utilis*. *J. Gen. Microbiol.* **129**, 965–971.

Bruinenberg, P. M., Jonker, R., van Dijken, J. P., and Scheffers, W. A. (1985). Utilization of formate as an additional energy source by glucose-limited chemostat cultures of *Candida utilis* CBS 621 and *Saccharomyces cerevisiae* CBS 8066. *Arch. Microbiol.* **142**, 302–306.

Flikweert, M. T., Kuyper, M., van Maris, A. J. A., Kötter, P., van Dijken, J. P., and Pronk, J. T. (1999). Steady-state and transient-state analysis of growth and metabolite production in a *Saccharomyces cerevisiae* strain with reduced pyruvate-decarboxylase activity. *Biotech. Bioeng.* **66**, 42–50.

Francois, J., and Parrou, J. L. (2001). Reserve carbohydrates metabolism in the yeast *Saccharomyces cerevisiae*. *FEMS Microbiol. Rev.* **25**, 125–145.

Frey, D. A., Fiaux, J., Szyperski, T., Wütrich, K., Bailey, J. B., and Kallio, P. T. (2001). Dissection of central carbon metabolism of hemoglobin-expressing *Escherichia coli* by ^{13}C nuclear magnetic resonance flux distribution analysis in microaerobic bioprocesses. *Appl. Environ. Microb.* **67**, 680–687.

Gírio, F. M., Roseiro, J. C., Sá-Machado, P., Duarte-Reis, A. R., and Amaral-Collaço, M. T. (1994). Effect of oxygen transfer rate on levels of key enzymes of xylose metabolism in *Debaryomyces hansenii*. *Enzyme Microb. Technol.* **16**, 1074–1078.

Gancedo, C., and Delgado, M. A. (1984). Isolation and characterisation of a mutant from *Saccharomyces cerevisiae* lacking fructose-1,6-bisphosphatase. *Eur. J. Biochem.* **139**, 221–225.

de Graaf, A. A., Striegel, K., Wittig, R. M., Laufer, B., Schmitz, G., Wiechert, W., Sprenger, G. A., and Sahm, H. (1999). Metabolic state of *Zymomonas mobilis* in glucose-, fructose-, and xylose-fed continuous cultures as analysed by ^{13}C- and ^{31}P-NMR spectroscopy. *Arch. Microbiol.* **171**, 371–385.

Granström, T., and Leisola, M. (2002). Controlled transient changes reveal differences in metabolite production in two *Candida* yeasts. *Appl. Microbiol. Biotechnol.* **58,** 511–516.

Granström, T., Ojamo, H., and Leisola, M. (2001). Chemostat study of xylitol production by *Candida guilliermondii*. *Appl. Microbiol. Biotechnol.* **55**, 36–42.

Granström, T. B., Aristidou, A. A., Jokela, J., and Leisola, M. (2000). Growth characteristics and metabolic flux analysis of *Candida milleri*. *Biotech. Bioeng.* **70**, 197–207.

van Gulik, W. M., and Heijnen, J. J. (1995). A metabolic network stoichiometry analysis of microbial growth and product formation. *Biotechnol. Bioeng.* **48**, 681–698.

Hallborn, J., Gorwa, M.-F., Meinander, N., Penttilä, M., Keränen, S., and Hahn-Hägerdahl, B. (1994). The influence of cosubstrate and aeration on xylitol formation by recombinant *Saccharomyces cerevisiae* expressing *XYL1* gene. *Appl. Microbiol. Biotechnol.* **42**, 326–333.

van Hoek, P., van Dijken, J. P., and Pronk, J. T. (1998). Effect of specific growth rate on fermentative capacity of Bakers's yeast. *Appl. Environ. Microb.* **64**, 4226–4233.

Jeppsson, H., Holmgren, K., and Hahn-Hägerdahl, B. (1999). Oxygen-dependent xylitol metabolism in *Pichia stipitis*. *Appl. Microbiol. Biotechnol.* **53**, 92–97.

de Jong-Gubbels, van Dijken, J. P., and Pronk, J. T. (1996). Metabolic fluxes in the chemostat cultures of *Schizosaccharomyces pombe* grown on mixtures of glucose and ethanol. *Microbiology* **142**, 1399–1407.

Kötter P., and Ciriacy, M. (1993). Xylose fermentation by *Saccharomyces cerevisiae*. *Appl. Microbiol. Biotechnol.* **38**, 776–783.

Nissen, T. L., Schulze, U., Nielsen, J., and Villadsen, J. (1997). Flux distribution in anaerobic, glucose-limited continuous cultures of *Saccharomyces cerevisiae*. *Microbiology* **143**, 203–218.

Oh, D.-K., Kim, S.-Y., and Kim J.-H. (1998). Increase of xylitol production rate by controlling redox potential in *Candida parapsilosis*. *Biotechnol. Bioeng.* **58**, 440–444.

Petersen, S., de Graaf, A. A., Eggeling, L., Möllneys, M., Wiechert, W., and Sahm, H. (2000). *In vivo* quantification of parallel and bidirectional fluxes in the anaplerosis of *Corynebacterium glutamicum*. *J. Biol. Chem.* **275**, 35 932–35 941.

Porro, D., Bianchi, M. M., Brambilla, L., Menghini, R., Bolzani, D., Carrera, V., Lievense, J., Liu, Chi, C.-L., Ranzi, B. M., Frontali, L., and Alberghina, L. (1999). Replacement of a metabolic pathway for a large-scale production of lactic acid from engineered yeasts. *Appl. Environ. Microb.* **65**, 4211–4215.

Postma, E., Verduyn, C., Scheffers, W. A., and van Dijken, J. P. (1989). Enzymic analysis of the Crabtree effect in glucose-limited chemostat cultures of *Saccharomyces cerevisiae*. *Appl. Env. Microbiol.* **55**, 468–477.

van Schaftingen, E., Hue, L., and Hers, H. G. (1980). Fructose-2,6-bisphosphate, the probable structure of the glucose- and glucagon-sensitive stimulator of phosphofructokinase. *Biochem. J.* **192**, 897–901.

Schmidt, K., Nielsen, J., and Villadsen, J. (1999). Quantitative analysis of metabolic fluxes in *Escherichia coli*, using two-dimensional NMR spectroscopy and complete isotopomer models. *J. Biotechnol.* **71**, 175–190.

Stephanopoulos, G., Aristidou, A. A., and Nielsen, J. (1998). ''Metabolic Engineering, Principles and Methodologies,'' p. 725, Academic Press, New York.

Vallino, J. J., and Stephanopoulos, G. (1993). Metabolic flux distributions in *Corynebacterium glutamicum* during growth and lysine overproduction. *Biotech. Bioeng.* **41**, 633–646.

Vandeska, E., Kuzmanova, S., and Jeffries, T. W. (1995). Xylitol formation and key enzyme activities in *Candida boidinii* under different oxygen transfer rates. *J. Ferment. Bioeng.* **80**, 513–516.

Verduyn, C., van Kleef, R., Frank, J., Schreuder, H., van Dijken, J. P., and Scheffers, W. A. (1985). Properties of the NAD(P)H-dependent xylose reductase from the xylose-fermenting yeast *Pichia stipitis*. *Biochem. J.* **226**, 669–677.

Verduyn, C., Postma, E., Scheffers, W. A., and van Dijken, J. P. (1990). Physiology of *Saccharomyces cerevisiae* in anaerobic glucose-limited chemostat culture cultures. *J. Gen. Microbiol.* **136**, 395–403.

Verduyn, C., Stouthamel, A. H., Scheffers, W. A., and van Dijken, J. P. (1991). A theoretical evaluation of growth yields of yeasts. *Antonic van Leeuwenhock*, 49–63.

Verduyn, C., Postma, E., Scheffers, W. A., and van Dijken, J. P. (1992). Effect of benzoic acid on metabolic fluxes in yeasts: a continuous culture study on the regulation of respiration and alcoholic fermentation. *Yeast* **8**, 501–517.

Wittman, C., Heinzle, E. (1999). Mass spectrometry for metabolic flux analysis. *Biotech. Bioeng.* **62**, 739–750.

Zupke, C., Sinskey, A. J., and Stephanopoulos, G. (1995). Intracellular flux analysis applied to the effect of dissolved oxygen on hybridomas. *Appl. Microbiol. Biotechnol.* **44**, 27–36.